

Protein Autoproteolysis: Conformational Strain Linked to the Rate of Peptide Cleavage by the pH Dependence of the N → O Acyl Shift Reaction

Denny G. A. Johansson,[†] Göran Wallin,[‡] Anders Sandberg,[†] Bertil Macao,[†] Johan Åqvist,[‡] and Torleif Hård^{*,†,§}

Department of Medical Biochemistry and Swedish NMR Centre, University of Gothenburg, Box 440, SE-405 30 Göteborg, Sweden, Department of Cell and Molecular Biology, Uppsala University, Box 596, SE-751 24 Uppsala, Sweden, and Department of Molecular Biology, Swedish University of Agricultural Sciences, Box 590, SE-751 24 Uppsala, Sweden

Received February 11, 2009; E-mail: torleif.hard@molbio.slu.se

Protein autoproteolysis is an intramolecular reaction in which the peptide chain is cleaved at a specific site. Most autoproteolytic and other protein-autoprocessing reactions involve an N → O (or N → S) acyl shift (also called acyl migration or rearrangement) of a peptide amide to form an ester.¹ With the notable exception of folded proteins, this reaction^{2,3} has never been observed at neutral pH, where instead the reverse O → N shift occurs rapidly.⁴ Scissile peptides in precursors of autoproteolytic proteins exhibit special properties.^{1,5–7} For instance, a nonplanar peptide in the glycosylasparaginase precursor⁷ acts to favor the ester in the N ⇌ O equilibrium.¹ Also, SEA domain autoproteolysis involves substrate destabilization by 7 kcal mol⁻¹, and molecular modeling and mutational analysis have indicated that conformational energy is dissipated as strain in the precursor.^{8–10} Still, the chemical mechanism by which strain is linked to acceleration of the N → O acyl shift has not been clarified. Here we show that it can be explained by a strain-dependent pK_a for amide nitrogen protonation. Conformational strain in combination with N → O acyl shift is therefore sufficient for autoproteolysis to occur at neutral pH in the absence of conserved features such as a catalytic triad or an oxyanion hole, which are not present at the SEA domain cleavage site.

The pH dependence of SEA domain autoproteolysis was studied in a slow-cleaving SEA mutant, because wild-type SEA undergoes rapid autoproteolysis during purification and rate measurements based on refolding¹⁰ do not allow for measurements below pH 6. The SEA 1G mutant contains a single glycine insertion to form a G₁₀₉₇G↓S₁₀₉₈VVV cleavage-site sequence, and autoproteolysis occurs immediately adjacent to the conserved serine (at the arrow), as in wild-type SEA.⁹ SEA 1G can be purified in partially (30–40%) cleaved form, and autoproteolysis can be followed as the reaction proceeds to completion by measuring the change in circular dichroism (CD) at 249 nm to monitor the formation of a proper protein core or by gel electrophoresis (SDS-PAGE) to directly observe cleavage products (Figure 1).

In analogy with the wild-type protein,¹⁰ SEA 1G autoproteolysis follows single-exponential kinetics. It is pH-dependent in the interval 3 to 8 with a maximum between pH 5 and 6 (*k*_{obs} ≈ 0.002 min⁻¹) corresponding to a half-life of ~6 h (Figure 2a). Autoproteolysis also occurs under alkaline conditions (not shown), but in that case it can proceed without N → O acyl shift, because a SEA 1G mutant that is incapable of acyl shift

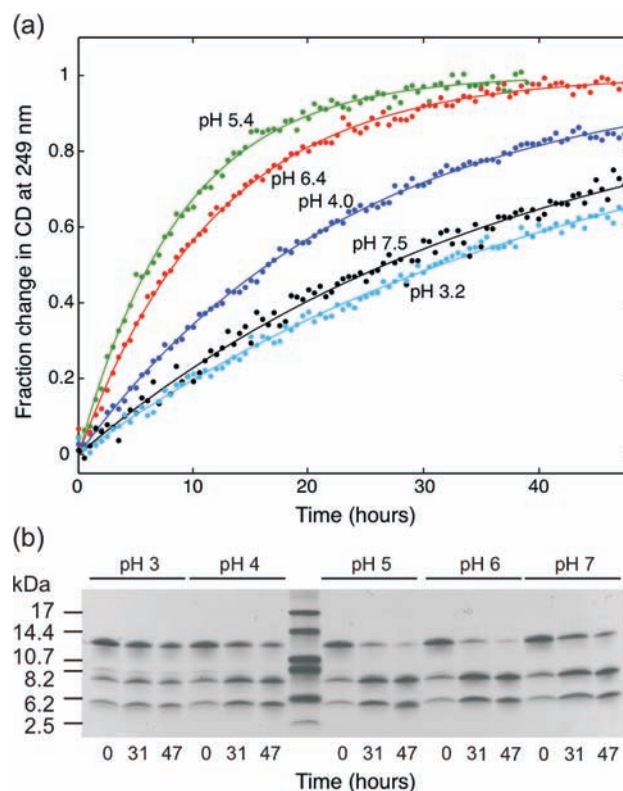


Figure 1. Autoproteolysis of SEA 1G. (a) Normalized change in CD at 40 °C and various pH values. Lines represent fits to a mono-exponential function. (b) SDS-PAGE of samples incubated at 30 °C. Molecular mass markers (middle lane) are indicated to the left. The band at ~14 kDa is uncleaved protein, while the bands at ~8 and ~6 kDa are autoproteolysis products. For experimental details, see the Supporting Information.

is still cleaved at high pH (Figure S1 in the Supporting Information). We attribute the high-pH cleavage to base-catalyzed amide hydrolysis, which in fact can also be promoted by conformational strain.¹¹

The bell-shaped pH dependence implies that autoproteolysis involves two protonation equilibria, one that becomes rate-limiting at high pH and the other at low pH. It is well-established that the N → O shift is acid-catalyzed,^{1,3} and we therefore assign it to depend on a protonation equilibrium constant *K*₁, which makes it rate-limiting at high pH. The rate-limiting step at low pH must be hydrolysis of the ester, since uncatalyzed ester hydrolysis is very slow,¹² whereas the rate of autoproteolysis of wild-type SEA is ~0.04 min⁻¹ at room temperature. However, ester hydrolysis can

[†] University of Gothenburg.

[‡] Uppsala University.

[§] Swedish University of Agricultural Sciences.

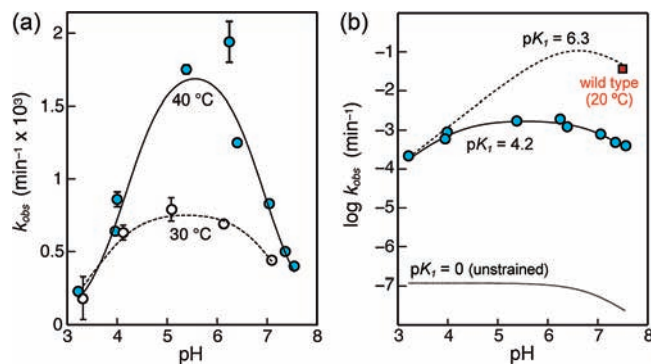
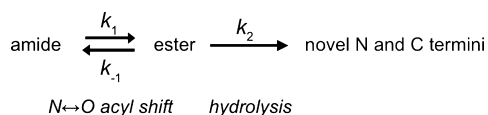


Figure 2. (a) Rate of SEA 1G autoproteolysis as a function of pH. Lines are fits to eq 1 with parameters for ester hydrolysis restrained to $pK_2 = 7$ and $k_2 > 0.02 \text{ s}^{-1}$. (b) Effect of pK_1 : data for SEA 1G ($pK_1 = 4.2$) are compared to expected rates for $pK_1 = 6.3$ and $pK_1 = 0$, with other kinetic parameters fixed according to the fit in (a) ($k_{1H}/k_{-1} = 20$ and $k_{2B} = 0.06 \text{ min}^{-1}$). If pK_1 represents amide nitrogen protonation, then variation of pK_1 as a function of amide strain provides a mechanistic link explaining the rapid autoproteolysis of wild-type SEA at neutral pH (indicated) as opposed to the lack of observable autoproteolysis in unstrained glycine–serine peptides.

reach such rates by intramolecular general base catalysis.^{13,14} In analogy, we expect hydrolysis to depend on the protonation state (equilibrium constant K_2) of the primary amine that is formed upon acyl shift. The autoproteolytic site is water-exposed on the protein surface,^{8,9} and pK_2 should therefore take a value between 7 and 8 (see ref 15).

If the protonation equilibria and interconversion of the intermediate are rapid, a kinetic analysis reduces to Scheme 1:

Scheme 1



Single-exponential kinetics is observed, and applying the steady-state approximation to the ester concentration yields

$$k_{\text{obs}} = \frac{k_2 k_1}{k_{-1} + k_2} = \frac{\left(k_{2B} \frac{K_2}{10^{-\text{pH}} + K_2} \right) \left(k_{1H} \frac{10^{-\text{pH}}}{10^{-\text{pH}} + K_1} \right)}{k_{-1} + \left(k_{2B} \frac{K_2}{10^{-\text{pH}} + K_2} \right)} \quad (1)$$

where rate constants are defined in Scheme 1 and the subscripts H and B indicate rates observed for the pure acid and base states of the amide and ester, respectively. Fitting eq 1 to the experimental data yields pK_1 values of 3.9 and 4.2 at 30 and 40 °C, respectively, and ester hydrolysis rate constant (k_{2B}) values of 0.04–0.06 min^{-1} when pK_2 is fixed at 7 and k_{2B} is required to take values greater than 0.02 min^{-1} (Figure 2).

Hence, the experimental data are consistent with a mechanism in which the initial N → O shift depends on a protonation event with an equilibrium constant K_1 that makes it rate-limiting for autoproteolysis at neutral pH. Further modeling of eq 1 shows that increasing pK_1 from ~4 (as determined here for SEA 1G) to 6.3 without changing the other parameters reproduces the rapid rate of autoproteolysis of wild-type SEA at pH 7.5 and that autoproteolysis would not be observable with $pK_1 < 0$ (Figure 2b).

We suggest that the protonation reflected in K_1 occurs at the amide nitrogen of the glycine–serine peptide bond in SEA. The pK_a for amide nitrogen protonation is very low (ca. -7 ; see ref 16), and unstrained peptides become protonated at the oxygen with $pK_a \approx 0$. However, studies of model compounds have shown that amide strain (twist) forces the nitrogen closer to sp^3 hybridization, with consequent loss of resonance stabilization and an increase in pK_a .^{11,17–20} Protonation by water or hydronium ion, as suggested for intein C-terminal cleavage,²¹ would also make the amide susceptible to nucleophilic attack at the carbonyl carbon by the conserved serine hydroxyl.¹¹

We used quantum-chemical calculations based on density functional theory and continuum solvent methods to further dissect such a mechanism for N → O shift (Figure 3a; see the Supporting Information for details).

First, we investigated whether straining the peptide moiety away from planarity would facilitate nucleophilic attack by the serine hydroxyl at an unprotonated ($-\text{NH}-$) amide (Figure 3b). We found that strain increases the substrate energy while the energies of conformations in which the serine hydroxyl and the carbonyl carbon are in close proximity remain constant, so the activation energy is indeed decreased as a result of substrate destabilization. However, the activation energies at all strain angles are still large, suggesting that strain alone is not sufficient to initiate the N → O acyl shift.

Second, we calculated the effect of strain on protonation (Figure 3c). The relations between twist (strain) and pK_a that have been observed with other models of twisted amides^{17–19} were readily reproduced in our peptide model: the pK_a values for nitrogen and oxygen protonation respond in opposite ways to strain, and nitrogen becomes the preferred site for protonation at a moderate nonplanarity (20°). In fact, as the H–N–C=O dihedral angle is decreased from 180 to 90°, the nitrogen pK_a changes continuously from -7.2 to >10 . The latter value is very close to that expected for fully sp^3 -hybridized secondary amines such as dimethylamine ($pK_a = 11$).

Third, we studied the effects of nucleophilic attack in a substrate in which the amide nitrogen is protonated ($-\text{NH}_2^+-$). The activation energy is now substantially reduced relative to the unprotonated case ($\sim 15 \text{ kcal/mol}$; Figure 3d) and close to the experimentally observed value (10 kcal/mol; ref 10). The calculations also suggest how the N → O acyl shift occurs: the peptide bond breaks as a consequence of ring strain imposed by the new oxygen–carbon bond in the hydroxyoxazolidine. A possible transition state for the reaction is shown in Figure 3a.

The pH dependence of SEA domain autoproteolysis and the results of quantum-chemical calculations are therefore consistent with a mechanism by which protein folding acts to distort the amide so the nitrogen can be protonated at neutral pH. Subsequent loss of peptide resonance stabilization allows for nucleophilic attack by the adjacent serine hydroxyl to transiently form a strained five-membered ring, which breaks up into an ester. The ester is then rapidly hydrolyzed, because the new amino group acts as a general base catalyst. The fact that distorted and/or unusual amides are also present in precursors of other proteins undergoing intramolecular acyl shifts^{1,5–7} suggests that this mechanism may be a common feature of protein autoprocessing.

Acknowledgment. This work was supported by the Swedish Research Council (VR) and the Swedish Strategic Research Foundation (SSF) Center MIVAC.

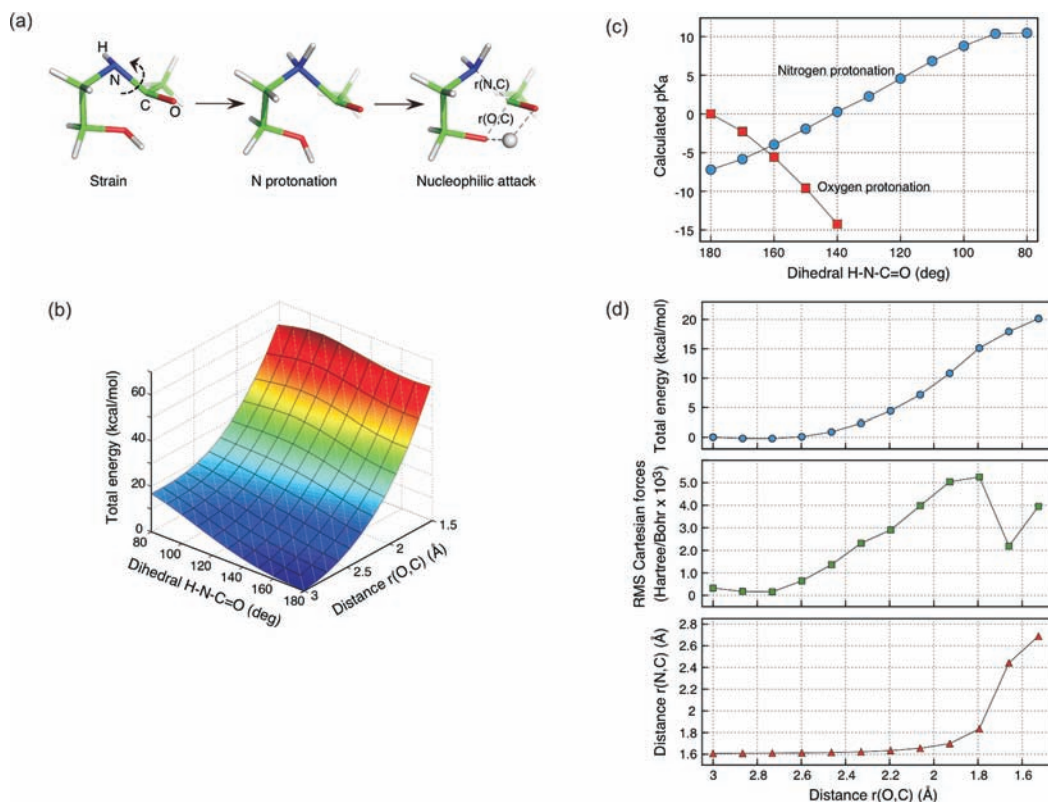


Figure 3. (a) Mechanism for N \rightarrow O acyl shift in SEA domain autoproteolysis. The molecule shown is a minimal representation of a glycine–serine dipeptide used for quantum-chemical calculations. Straining of the peptide bond (left) distorts it from planarity. The subsequent loss of resonance stabilization increases the pK_a for nitrogen protonation (middle), which in turn facilitates nucleophilic attack of the serine hydroxyl on the carbonyl carbon (right). The structure at the right is a possible transition state for the N \rightarrow O shift (see the Supporting Information). (b–d) Results of quantum-chemical calculations. (b) Nucleophilic attack at the carbonyl carbon by the hydroxyl oxygen in the absence of protonation. The surface shows the total energy at constrained values of the carbon–oxygen distance $r(O,C)$ and the H–N–C=O dihedral angle. (c) pK_a values for protonation of nitrogen and oxygen as functions of strain. Calculated ΔpK_a values (see the Supporting Information) were referenced to known values for oxygen protonation^{22,23} ($pK_a = 0$) and nitrogen protonation ($pK_a = -7.2$, calculated according to Fersht¹⁶) in an unstrained peptide. (d) Nucleophilic attack at the carbonyl carbon by the hydroxyl oxygen with the amide nitrogen protonated and in an sp^3 configuration. The graph shows (top) the total energy, (middle) the forces acting on all of the atoms, and (bottom) the peptide bond length $r(N,C)$ as functions of the oxygen–carbon distance $r(O,C)$. The dependence of the Cartesian forces on the nucleophilic-attack distance reflects the buildup of ring strain, which is released as the peptide bond breaks.

Supporting Information Available: Materials and Methods, two figures, and references. This material is available free of charge via the Internet at <http://pubs.acs.org>.

References

- (1) Paulus, H. *Chem. Soc. Rev.* **1998**, *27*, 375–386.
- (2) Bergmann, B.; Brand, E.; Weinmann, F. *Hoppe-Seyler's Z. Physiol. Chem.* **1923**, *131*, 1–17.
- (3) Iwai, K.; Ando, T. *Methods Enzymol.* **1967**, *11*, 263–282.
- (4) Shao, Y.; Paulus, H. *J. Peptide Res.* **1997**, *50*, 193–198.
- (5) Klabunde, T.; Sharma, S.; Telenti, A.; Jacobs, W. R.; Sacchettini, J. C. *Nat. Struct. Biol.* **1998**, *5*, 31–36.
- (6) Romanelli, A.; Shekhtman, A.; Cowburn, D.; Muir, T. W. *Proc. Natl. Acad. Sci. U.S.A.* **2004**, *101*, 6397–402.
- (7) Xu, Q.; Buckley, D.; Guan, C.; Guo, H.-C. *Cell* **1999**, *98*, 651–661.
- (8) Macao, B.; Johansson, D. G.; Hansson, G. C.; Härd, T. *Nat. Struct. Mol. Biol.* **2006**, *13*, 71–76.
- (9) Johansson, D. G. A.; Macao, B.; Sandberg, A.; Härd, T. *J. Mol. Biol.* **2008**, *377*, 1130–1143.
- (10) Sandberg, A.; Johansson, D. G. A.; Macao, B.; Härd, T. *J. Mol. Biol.* **2008**, *377*, 1117–1129.
- (11) Lopez, X.; Mujika, J. I.; Blackburn, G. M.; Karplus, M. *J. Phys. Chem. A* **2003**, *107*, 2304–2315.
- (12) Mabey, W.; Mill, T. *J. Phys. Chem. Ref. Data* **1978**, *7*, 383–415.
- (13) Bruice, P. Y.; Bruice, T. C. *J. Am. Chem. Soc.* **1974**, *96*, 5523–5532.
- (14) Fife, T. H.; Singh, R.; Bembli, R. *J. Org. Chem.* **2002**, *67*, 3179–3183.
- (15) Tanford, C. *Adv. Protein Chem.* **1962**, *17*, 69–165.
- (16) Fersht, A. R. *J. Am. Chem. Soc.* **1971**, *93*, 3504–3515.
- (17) Wang, Q. P.; Bennet, A. J.; Brown, R. S.; Santasiero, B. D. *J. Am. Chem. Soc.* **1991**, *113*, 5757–5765.
- (18) Greenberg, A.; Moore, D. T.; Dubois, T. D. *J. Am. Chem. Soc.* **1996**, *118*, 8658–8668.
- (19) Mujika, J. I.; Mercero, J. M.; Lopez, X. *J. Phys. Chem. A* **2003**, *107*, 6099–6107.
- (20) Choo, S. J.; Cui, C.; Lee, J. Y.; Park, J. K.; Suh, S. B.; Park, J.; Kim, B. H.; Kim, K. S. *J. Org. Chem.* **1997**, *62*, 4068–4071.
- (21) Shemella, P.; Pereira, B.; Zhang, Y.; Van Roey, P.; Belfort, G.; Garde, S.; Nayak, S. K. *Biophys. J.* **2007**, *92*, 847–853.
- (22) Gillespie, R. J.; Birchall, T. *Can. J. Chem.* **1963**, *41*, 148–155.
- (23) Martin, R. *J. Chem. Soc.* **1972**, 793–794.

JA9010817